CRYSTAL GROWTH & DESIGN

pubs.acs.org/crystal

Article

Overgrowth of Protrusion Defects during Sublimation Growth of Cubic Silicon Carbide Using Free-Standing Cubic Silicon Carbide Substrates

Michael Schöler, Francesco La Via, Marco Mauceri, and Peter Wellmann*

Cite This: https://doi.org/10.1021/acs.cgd.1c00343

Read Online

ACCESS | Metrics & More | Article Recommendations

ABSTRACT: We investigated the overgrowth of protrusion defects during sublimation growth of cubic silicon carbide (3C-SiC) using free-standing on-axis and off-axis substrates. Three different overgrowth mechanisms were found to contribute to defect elimination: (i) mutual overgrowth by defects of the same type, (ii) real overgrowth by step-flow growth, and (iii) overgrowth by quasi-step-flow growth at surface irregularities. Mechanisms (i) and (iii) are not real overgrowth mechanisms because they are directly linked to the inducing defects themselves or other undesired disturbances of the substrate. However, at high defect densities or for the on-axis substrate, they represent a relevant elimination mechanism. Overgrowth according to (ii) is possible only for off-axis substrates and represents a real elimination mechanism, leading to an improvement of the material quality. In the context of this work, we provide a phenomenological description of the overgrowth principle as well as limitations for the defect elimination, depending on the structure of the protrusions. For the first time, the overgrowth of protrusions has been categorized for different types and qualities of substrates. Fundamental differences were identified, which can lead to a more focused further development of defect elimination in 3C-SiC.

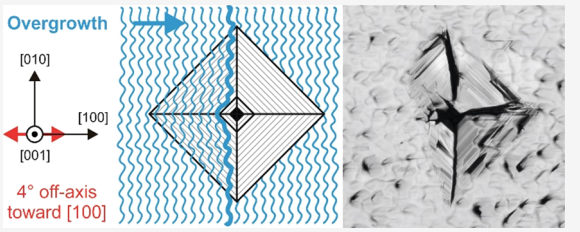

INTRODUCTION

Silicon carbide (SiC) has been established as irreplaceable material system for power electronics. Its success is due to its outstanding physical properties, such as a wide band gap, high breakdown field strength, high thermal conductivity, and chemical as well as radiation resistance. Currently, the hexagonal silicon carbide modifications (4H- and 6H-SiC) are used almost exclusively. 4H- and 6H-SiC can be grown using the physical vapor transport (PVT) method, which can be considered as a mature standard method to produce high-quality SiC single crystals. Hence, 4H- and 6H-SiC materials are available in sufficient quantities. However, hexagonal polytypes also have some disadvantages, especially for applications in metal-oxide semiconductor (MOS) devices like MOS field-effect transistors (MOSFETs). For MOSFETs, defect states typically form at the interface between the semiconductor and the oxide. Because of the wide band gap, these defects states are located within the band gap for 4H- and 6H-SiC, where they can act as so-called near-interface-traps (NITs)[1] and reduce the channel mobility of MOSFETs. The cubic modification of SiC should be advantageous for these applications. Cubic silicon carbide (3C-SiC) has the smallest band gap among all SiC polytypes with 2.39 eV.[2] Defect states at the 3C-SiC/SiO_2-interface therefore lie within the conduction band where they have hardly any influence on the channel mobility.[3] 3C-SiC therefore has great potential for MOSFETs, although the range of applications is limited by the smaller band gap to medium voltages up to approximately 800 V.[4−6] However, compared to the hexagonal polytypes, the fabrication of 3C-SiC is still a major challenge. After initial approaches with sublimation methods,[7−9] the focus has changed on the development of the heteroepitaxial growth of 3C-SiC on silicon substrates since the early 1980s.[10] Although remarkable progress has been made in recent years, high defect densities and high stress in the material hinder large-scale technical use.[11−14]

Sublimation methods could play an important role in overcoming these obstacles. It has already been shown that stress in the 3C-SiC-on-Si material can be significantly reduced by subsequent homoepitaxial growth.[15] Similarly, a decrease of the stacking fault (SF) density during the growth of thick layers has been documented.[16] In addition to SFs, protrusion defects are one of the major problems equally for the use of the material and for the fabrication of bulk crystals. Although there are reports about the reduction of defect density,[17] complete

Received: March 27, 2021
Revised: May 17, 2021

elimination or a corresponding mechanism has not yet been described. The present work picks up here and shows both the growth mechanism and an associated mechanism for the overgrowth of the protrusion defects.

EXPERIMENTAL DETAILS

The 3C-SiC layers were grown using the sublimation method using a sublimation-sandwich approach.[7−9,16,18,19] Figure 1 depicts the

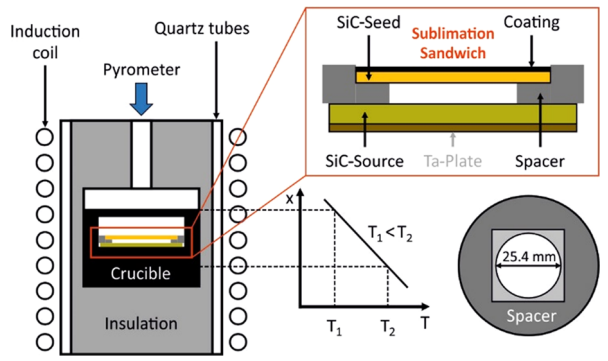

Figure 1. Schematic of the setup for the fabrication of 3C-SiC layers by sublimation growth. All the major components of the growth setup are depicted. Moreover, a magnified view of the sublimation sandwich is shown. Indicated is the temperature gradient on the growth cell, which is the driving force for crystal growth. Circular spacers were used to produce layers with a diameter of 1 inch.

schematic illustration of the growth setup used in this work. The main component of the growth setup is the hot zone, which contains the sublimation sandwich. The most important feature is the small distance between the source and the seed, which is set by graphite spacers with a thickness of typically 0.75 to 1.00 mm. This structure of the growth cell allows to achieve high-temperature gradients and thus high supersaturation, which are the fundamental prerequisites for the stable growth of 3C-SiC.[20] The hot zone is realized in an inductively heated state-of-the-art PVT reactor with double-walled and water-cooled quartz tubes. The hot zone with graphite crucible is surrounded with an insulation material. The relative position of the coil and the hot zone forces a vertical temperature gradient on the growth cell, which is the driving force for mass transport and crystal growth at the seed.

Free-standing 3C-SiC layers provided by LPE Epitaxial Technology Center in Catania were used as the seed layers for sublimation growth. The layers were pieces from 4 inch or 6 inch wafers with a thickness of 70−240 μm. Within the scope of this work, both on-axis and off-axis (100)3C-SiC seed layers were investigated. The off-axis layers exhibit a tilt of 4° toward the [110] or [100] direction. The study of the growth and defect elimination mechanisms was performed focusing on the tilting toward [100]. The seed layers were produced by chemical vapor deposition (CVD) on silicon substrates and subsequent melting of silicon, which was carried out by the supplier. All seed layers for sublimation growth were prepared from the 4-inch and 6-inch wafers using laser ablation[21,22] as the separation mechanism. The seeds were cut into square pieces of approximately 26.8 × 26.8 mm^2, according to the recess in the spacer, as shown in Figure 1. Subsequently, the growth of circular 3C-SiC layers with a diameter of 1 inch was performed on the seed layers. To protect the backside of the seed from sublimation, it was coated with a backside coating of carbon (C) or tantalum (Ta). Polycrystalline SiC wafers produced in our own laboratory were used as the source material. Underneath the source was a tantalum foil, which acts as a carbon getter during growth and shifts the gas-phase composition in favor of silicon, which additionally stabilizes the growth of 3C-SiC.[20] Crystal growth was performed at temperatures between 1950−2000 °C. The temperature was measured using a two-color pyrometer on the crucible lid, with the measured temperature being about 50 °C lower than the growth temperature at the seed. Depending on the growth temperature and the process duration, the average growth rate varied in the range 150−230 μm/h. For the investigated parameter range, no influence on the layer quality or the elimination of defects could be determined by the variation of the growth parameters.

RESULTS AND DISCUSSION

Attempts to grow thick 3C-SiC layers by sublimation growth currently led to the situation illustrated in Figure 2. Because of

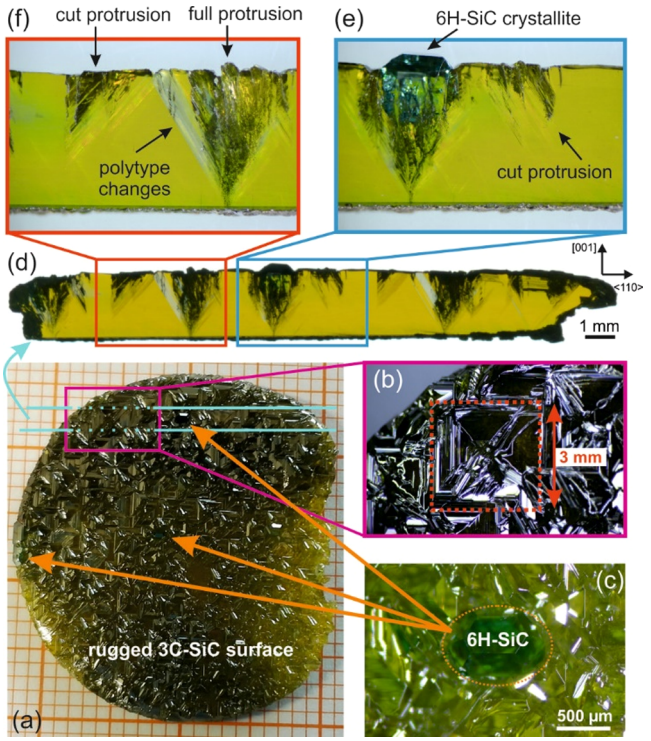

Figure 2. 3C-SiC crystal with a thickness of (2340 ± 40) μm. (a) Top view of the surface rugged by protrusion defects. (b) Individual protrusions together with their flanks can reach an edge length of up to 3 mm. (c) Rugged surface causes the nucleation of hexagonal SiC on {111} surfaces. (d) In the cross-section, center-cut protrusion defects are visible as dark, funnel-shaped structures. Protrusions cut off center are only partially visible and do not appear to start at the original Si/3C-SiC interface. (e) Magnified view of a 6H-SiC crystallite formed on a protrusion defect. (f) Magnified view of a polytype change (transparent) formed around protrusion defects.

high defect densities with protrusion defects being the main reason, the quality of the crystal deteriorates significantly within a few millimeters of growth. Figure 2a-f shows a 2.34 mm thick 3C-SiC layer. The protrusion density of the used seed layer can be described as typical for the currently available material. It was not possible to determine the exact defect density of the seed layer because the protrusions on the 72 μm thick, free-standing seed layer could not be clearly identified. In addition, the local defect density on the 6-inch donor wafer varied significantly in some cases so that the specification of an average value for the 1-inch samples was not useful. However, the example clearly shows the limitation resulting from the protrusion defects. With increasing 3C-SiC thickness, the protrusions expand vertically and horizontally. Although this results in defect reduction by mutual overgrowth, the overall crystal quality is not improved because the surviving defects

https://doi.org/10.1021/acs.cgd.1c00343
Cryst. Growth Des. XXXX, XXX, XXX−XXX

cover the entire surface (Figure 2a). In the example shown, individual protrusions may obtain an edge length of approximately 3 mm, including the surrounding defective areas (Figure 2b).

In the context of a defective core of the protrusions, the lateral expansion of these defects lead to a rugged surface, as can be seen in Figure 2a-d. The rugged surface can result in a loss of 3C-SiC polytype information for the incoming gas species during the subsequent sublimation growth process. For example, the protrusion flanks formed by the stacking faults in (111) planes may be more likely to provide the seed information for the nucleation of hexagonal SiC on the equivalent {0001} faces, as can be seen in Figure 2c and e. The lateral expansion of the protrusions arises from the cross-sectional views shown in Figure 2d–f. In addition to the expansion, the formation of polytype changes can also be observed in the surroundings of protrusions, as illustrated in Figure 2f. It follows that protrusion defects are one of the major obstacles for the fabrication of 3C-SiC bulk crystals. The overgrowth of protrusions observed for the off-axis 3C-SiC substrates could lead to a substantial improvement of the crystal quality. In this work, fundamental mechanisms are presented.

Off-oriented 3C-SiC layers typically exhibit a macroscopically smooth but textured surface. Figure 3 depicts a 436 μm thick (100)3C-SiC layer which is 4° off-axis toward the [100] direction. In Figure 3a, the textured surface is clearly visible. The rectangular disturbances on the surface are protrusion defects shown in the enlarged image (c). These defects will be discussed in detail below. The second enlarged view (b) shows the surface morphology of the layer.

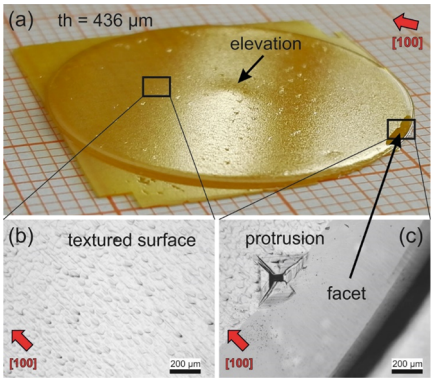

Figure 3. Surface morphology of the off-axis 3C-SiC layers. (a) Lateral view of a 1 inch specimen with typical textured surface and the formation of a facet at the edge of the layer. (b) Enlarged view of macroscopically textured surface with a scalelike structure. (c) Enlarged view of the edge region showing the facet and a protrusion defect. The red arrows indicate the direction and orientation of the step flow.

The surface texture of the off-axis layers originates from the microstructure and the growth mechanism. Growth on off-oriented substrates usually follows the step-flow mechanism. Because of substrate tilting, growth occurs at growth steps along the tilting direction. In the case of 3C-SiC, the surface morphology exhibits a scalelike structure of macro steps, as can be seen from the enlarged view in Figure 3b. These macro steps are in turn built up from the growth steps, as shown in the atomic force microscopy (AFM) image in Figure 4. This surface morphology is referred to as the "zig-zag" morphology in the literature for 3C-SiC.[23]

The (100)-oriented layer shown in Figure 3a exhibits tilting along the [100] direction. Accordingly, growth steps also run in this direction. The same applies to the superstructure of the macro steps, resulting in the texture shown in Figure 3b. When growing on tilted substrates, the formation of a facet at the edge of the sample is observed (c). The position of the facet correlates with the substrate and tilting orientation. The enlarged view in Figure 3c shows the transition area between the textured surface and facet. Directly at the transition, there is a protrusion defect from which the inclination of the tilted facet surface emerges. During the preparation of tilted layers, another peculiarity was observed. For all the layers, the formation of an elevation in the center of the sample could be observed. This is due to a locally increased growth rate because the same structure is found as deepening in the crystalline SiC source material like a negative structure (not shown). Regarding the surface structure and crystallinity, no differences were found compared to the surrounding areas. The reason for the formation of this anomaly could not be clarified so far. A connection with the off-orientation of the layer is probable because this effect could not be observed for on-axis layers.

The schematic in Figure 5 illustrates the growth mechanism of 3C-SiC on tilted substrates and the formation of a textured surface morphology, as described above.

The smallest surface structural unit is the growth step with a length of about 100–900 nm. The macro steps are built from these smallest units. As indicated in the schematic in Figure 5 and in the AFM image in Figure 4, the length of the growth steps is also determined by the superstructure of the macro steps. In areas with higher curvature, for example, at the peak of a macro step, the growth step length is typically between 500 and 900 nm because of step bunching. In contrast, the step length is significantly shorter at 100 to 200 nm at the flanks of the macro steps. The flanks exhibit a higher macroscopic inclination, which leads to shorter steps and a more uniform distribution of the step length.

The length of the macro steps is about 30 to 50 μm. Similar to the growth steps, the morphology of the macro steps is also dependent on the global superstructure. In the case of macro steps, the curvature of the substrate corresponding to the shape of the isotherms in the growth cell represents the underlying superstructure. This leads to the fact that the closer the steps are to the edge of the layer, the larger is the height or maximum height difference of the macro steps. Typically, the height is 350–500 nm.

Overall, it can be concluded that the growth on the tilted substrates leads to favorable growth conditions. Even for longer growth times and thicker 3C-SiC layers, no fundamental change in the growth mechanism or surface morphology was observed. Figure 6a shows exemplary surface areas of 3C-SiC layers with 436, 623, and 777 μm thickness. While the surface morphology shows no changes, the dimension of the pyramidal protrusion defects increases. The lateral expansion of these defects with increasing layer thickness is related to the structure of this defect and has been described in previous studies.[24,25]

Protrusion defects represent one of the major challenges in exploiting the 3C-SiC material system. The origin of these defects is due to the fabrication of the seed layers for sublimation growth. The seed layers used in this work were fabricated in a CVD process by heteroepitaxial deposition on

https://doi.org/10.1021/acs.cgd.1c00343
Cryst. Growth Des. XXXX, XXX, XXX–XXX

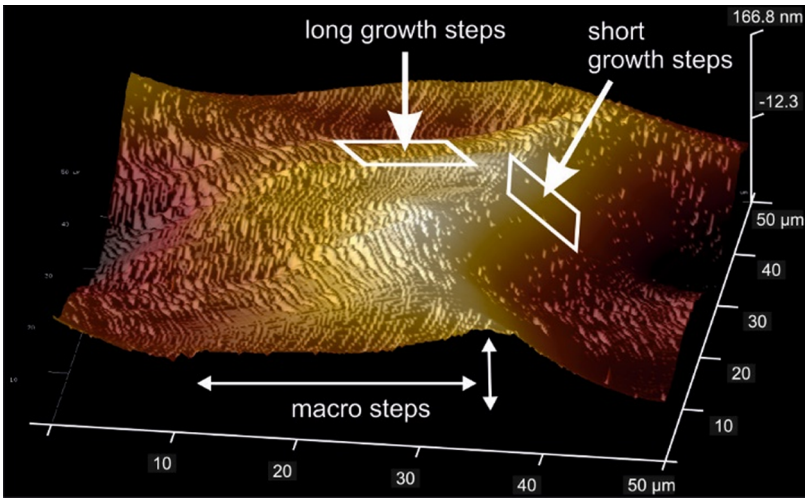

Figure 4. AFM image of a surface region of an off-axis 3C-SiC layer showing the development and formation of the scalelike texturing from macro steps. The macro steps build up from the growth steps of the step flow. The markings point to areas that typically have long and short steps, respectively. In addition, the length and height of the macro steps is indicated.

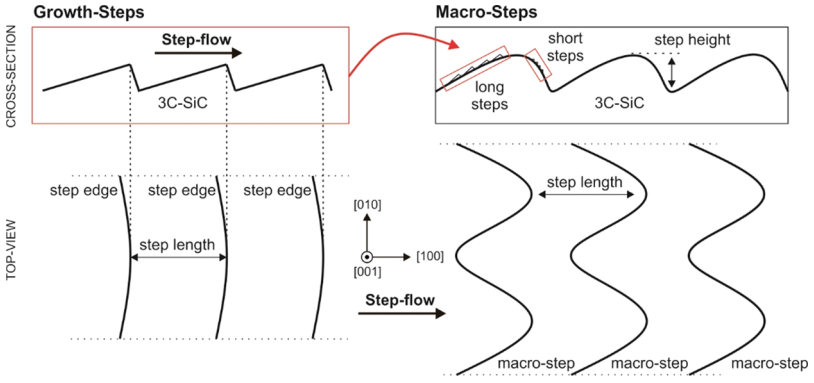

Figure 5. Schematic of the surface morphology with step-flow growth on the tilted 3C-SiC layers. The schematic shows as an example tilting toward the [100] direction so that the step edges also move in the [100] direction. The surface structure of the tilted layers shows a meandering superstructure of macro steps. These build up from the growth steps. The growth steps in turn exhibit different surface morphologies depending on the topography of the macro steps. The schematic is used to illustrate the 3C-SiC growth mechanism on tilted substrates and to define the terms used.

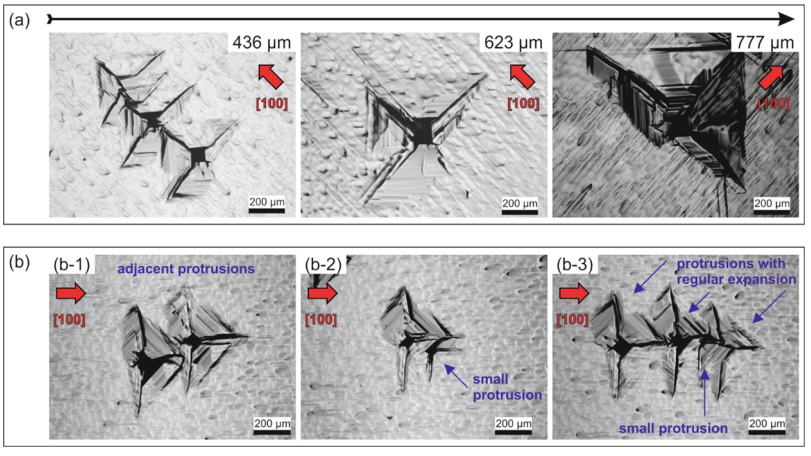

Figure 6. Surface morphology and defects in (100)3C-SiC 4° off-axis toward [100]. (a) Surface morphology and expansion of protrusion defects with increasing layer thickness. (b) Defect elimination mechanism by the mutual overgrowth of protrusions and the formation of new protrusions within the proximity of already-existing protrusion defects. The red arrows indicate the direction and orientation of the step flow.

silicon substrates. In this process, the protrusion defects form during the initial stage of deposition at the interface between silicon and 3C-SiC. Structurally, the protrusions consist of a polycrystalline or defect-rich single-crystalline SiC core surrounded by stacking faults in the (111) planes.[26−28] This structure gives rise to the pyramidal shape of the defect.

https://doi.org/10.1021/acs.cgd.1c00343
Cryst. Growth Des. XXXX, XXX, XXX−XXX

Starting from the point of formation, the defects continue to expand.

The full elimination of these defects during sublimation growth has not yet been demonstrated. However, a partial reduction of the protrusion density by overgrowth is reported.[17] The underlying mechanism has not yet been clearly described.

In this work, three fundamental mechanisms were found that can lead to protrusion overgrowth: (i) mutual overgrowth by adjacent protrusions, (ii) real overgrowth due to the step-flow mechanism for off-axis substrates, and (iii) quasi-step-flow overgrowth on surface irregularities. Mutual overgrowth according to (i) can be considered as one of the most common elimination processes. Especially at high defect densities, adjacent protrusions are close to each other. With increasing layer thickness during growth, this will lead to intergrowth and thus overgrowth, as can be seen from the images shown in Figure 6b. Furthermore, the formation of protrusions within the proximity of already-existing protrusions can be detected (Figure 6 b-2). This effect can be recognized by the fact that newly formed protrusions are significantly smaller than the protrusions that formed at the Si/SiC interface during the initial stage of the CVD growth. The formation of new protrusions can be attributed to the disturbed crystal regions in the vicinity of the already-existing protrusions. Figure 6(b-2) and (b-3) show the overgrowth of such smaller defects by the protrusions of regular size. Mutual overgrowth is not a real overgrowth mechanism because elimination occurs by the interaction of defects of the same type. For this reason, this mechanism cannot lead to a complete elimination of protrusions. With increasing crystal thickness, the nominal defect density decreases as several individual defects merge and appear as single defect structures. In addition, the mechanism works only for high defect densities or local accumulations of defects. Therefore, the defect elimination process is due to the quality of the currently available seed layers themselves and would be neither possible nor necessary if the protrusion density of the substrate is significantly lower. The surviving protrusions expand with the layer thickness and negatively affect the material quality.

The real overgrowth of protrusions according to (ii) is directly related to the step-flow growth on the tilted substrates. Partially overgrown protrusions can typically be observed on the surface of the off-axis layers, as depicted in Figure 6a. In terms of their external shape, protrusions can be approximately compared to flat pyramids. In the case of tilted substrates, the protrusions can be overgrown starting from the edge regions because of the step flow with increasing layer thickness. The mechanism is presented here as examples in Figure 7 using a microscope and AFM images. Here, (a) shows an outer edge region of a protrusion, while (b) shows an area near the center of a protrusion. Because of the step flow on the off-axis substrates, the growth steps run on the protrusion flanks and thereby overgrow the defects layer by layer. This happens until the protrusion is completely overgrown. A flat and smooth protrusion flank and a weakly pronounced core is favorable for the overgrowth mechanism. In (c), an already overgrown area of a protrusion is shown. The surface morphology in this area is indistinguishable from the surface in areas without protrusions. It follows that the protrusions are overgrown by the crystal regions of high crystallinity.

The efficiency of the overgrowth depends on the structure and composition of the protrusions. In addition to the defect

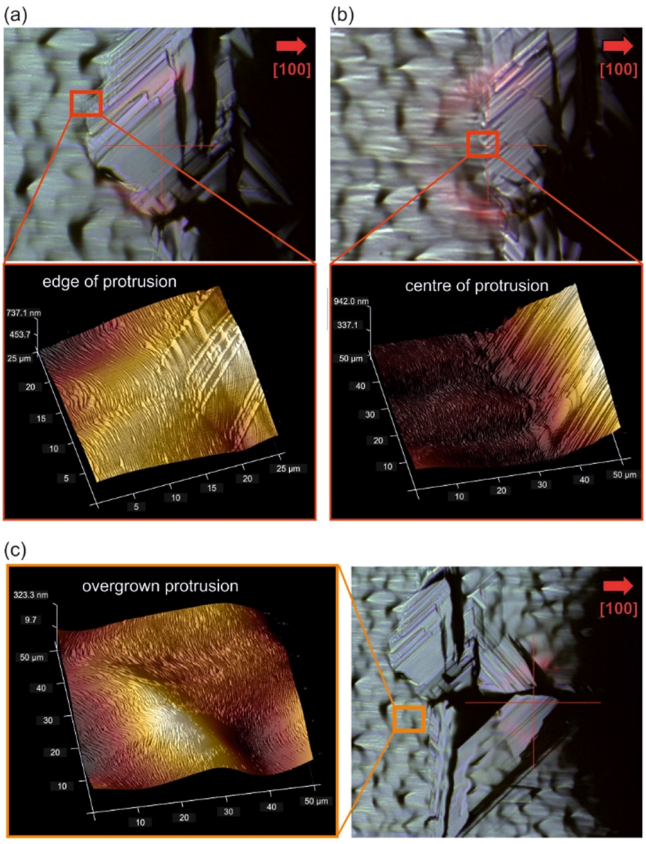

Figure 7. Overgrowth mechanism of protrusion defects on the tilted 3C-SiC layers. (a) Overgrowth in an area with a small height difference between the surrounding area and the defect. (b) Overgrowth or pile-up of growth steps in an area with a large height difference at a steep protrusion flank. (c) Surface morphology in an area above a partially overgrown protrusion. The red arrows indicate the direction and orientation of the step flow.

flanks, the core is one of the most striking features of the protrusions. In the literature, several different explanations of the structure of this core exist. Accordingly, the character of the core is attributed to polycrystalline, twinned, or even amorphous SiC.[26−28] Most likely, all the descriptions are valid, and different structures exist. This is consistent with the empirical results, according to which the appearance of protrusions differs considerably. In particular, the appearance of the core varies significantly. Depending on how pronounced it is, the overgrowth of the protrusion is affected accordingly.

Experimental evidence for the existence of different protrusion structures and different velocities of overgrowth is given in Figure 8. Figure 8a shows protrusions which are overgrown along the [100] direction up to approximately the center or core of the defect. In addition to that, the overgrowth beyond the center of the protrusion can be observed, as indicated in Figure 8b and c. Finally, complete overgrowth can also be observed, in which the protrusion is no longer visible on the surface, except for small inhomogeneities at the former edges. Because all images in Figure 8 show similar-sized protrusions and were taken on the surface of the same 3C-SiC layer, the differently overgrown protrusions depicted cannot represent different phases of one and the same overgrowth mechanism. Rather, this is evidence that the efficiency of overgrowth depends on the structure of the protrusion.

https://doi.org/10.1021/acs.cgd.1c00343
Cryst. Growth Des. XXXX, XXX, XXX−XXX

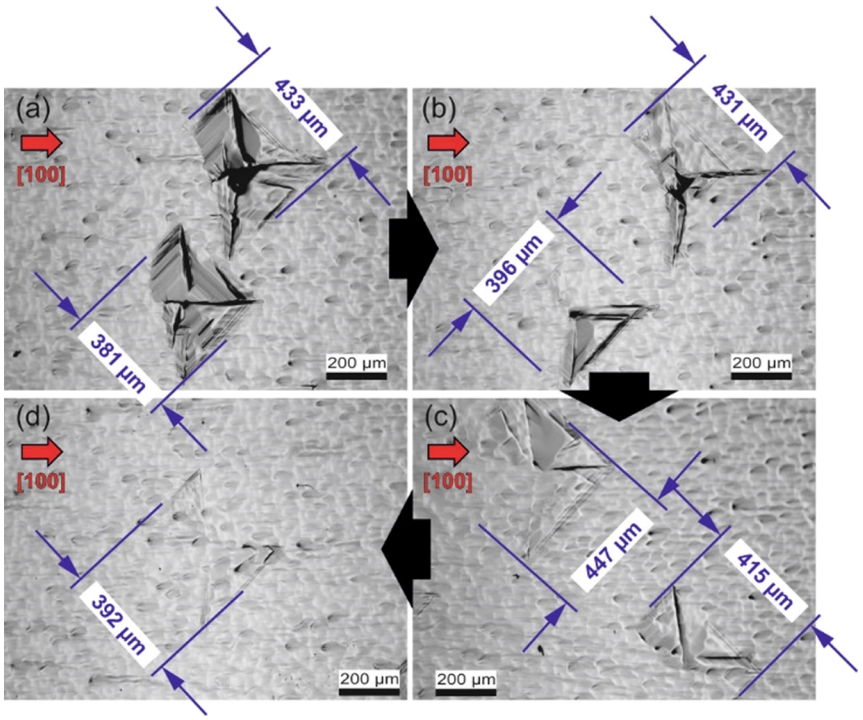

Figure 8. Overgrowth of protrusions on the (100)3C-SiC layers 4° off-axis toward [100]. (a) Typical visual appearance of protrusion defects. The protrusions are partially overgrown by the surrounding material up to approximately the center or the core of the defect. (b, c) Overgrowth of protrusions beyond the center of the defect. (d) Complete overgrowth of a protrusion. The red arrows indicate the direction and orientation of the step flow.

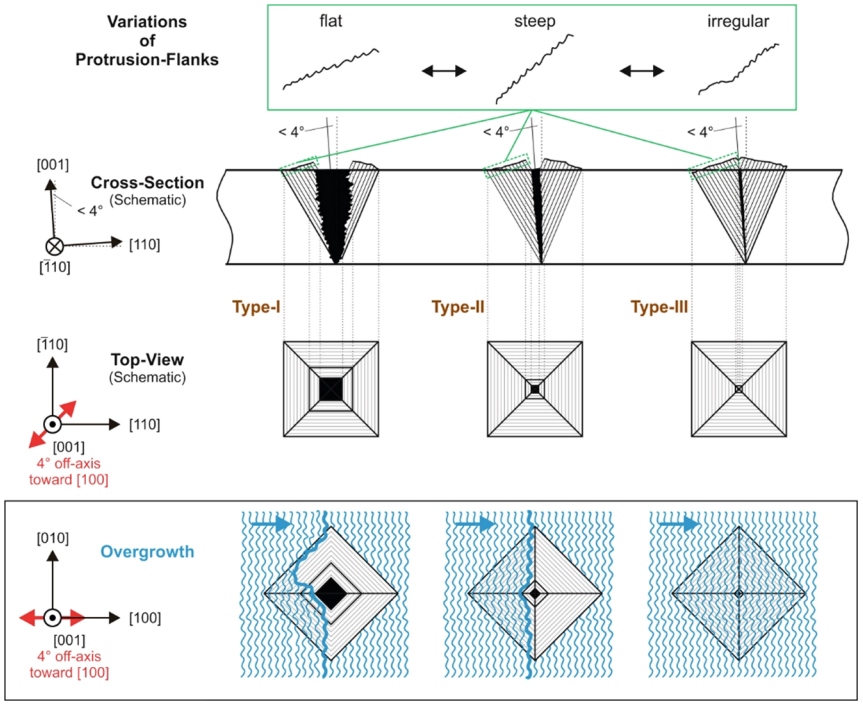

Figure 9. Classification of protrusions into three types based on empirical results with respect to the appearance of the defect and the observed overgrowth mechanism. Type-I protrusions have a large, pronounced core that represents a barrier to the step-flow growth. Therefore, type-I protrusions can be overgrown at maximum up to half of the defect. Type-II protrusions largely correspond to type-I, although the core is significantly smaller than that in type-I. These defects are usually overgrown by half, with the core remaining apparent. Type-III protrusions have a very small or even no core and may become completely overgrown. In addition to the three different types of protrusions, further structures exist, as well as variations that differ, for example, in the structure of the protrusion flank, as depicted in the schematic. The blue arrows in the "overgrowth" line indicate the orientation of the step flow. The tilting is schematically indicated in the figures and illustrated by red arrows.

https://doi.org/10.1021/acs.cgd.1c00343
Cryst. Growth Des. XXXX, XXX, XXX−XXX

Based on the observed overgrowth scenarios, the protrusions were classified into three main groups that can be overgrown to different degrees. In Figure 9, a schematic is given which provides an overview of the various types of protrusions as well as their orientation, structure, and overgrowth scenarios. The key feature is the core of the protrusion which emerges from the cross-sectional view. According to the structure and dimension of the core, the protrusions can be classified into three different groups. Type-I represents defects with a large and pronounced core. These defects are typically overgrown to no more than the center of the protrusion, with the core being an obvious barrier for the step flow. Type-II defects are characterized by a much smaller core. As a result, the defects are typically overgrown up to the center. Protrusions that have no or a barely pronounced core are classified as type-III. These protrusions can be overgrown completely by the step-flow mechanism. In addition to the different emphasis of the core, the protrusion flanks may be different for all three types. This also affects the efficiency of the overgrowth. In general, the flatter the protrusion side surface, the easier and faster the defect can be overgrown.

The previous explanations specifically referred to growth on the tilted substrates. However, there is a third mechanism leading to the overgrowth according to (iii) which can be considered as the quasi-step-flow overgrowth. While the principle of overgrowth is the same as in (ii), the origin is not due to general substrate tilting but to localized surface irregularities. These irregularities also lead to local substrate tilting and, therefore, to the growth according to the step-flow mechanism. These irregularities can be caused by process-related effects or by defect structures such as protrusions on the substrate surface. For example, it can be assumed that the overgrowth of protrusions observed on on-axis substrates[17] is a process-induced effect which can be attributed to irregularities caused by the attachment of the seed layer with a glue layer.[16] In contrast to this, Figure 10a shows quasi-step-flow growth on the on-axis substrates at irregularities caused by the clusters of protrusion defects. In comparison, Figure 10b depicts growth on the on-axis substrates without surface irregularities and, hence, without pronounced step-flow growth and without the formation of macro steps.

All overgrowth mechanisms lead to a reduction of the protrusion density. However, the efficiency and usability are very limited for (i) and (iii). In (i), defect reduction basically works only in the presence of high defect densities, which counteracts the actual aim of the low defect densities. The mechanism in (iii), on the other hand, is not directly controllable, and inhomogeneities also negatively affect the crystal quality. It follows that (ii) is the only mechanism that can lead to a real reduction of the protrusion density independent of the defect density and that is based on the real overgrowth principle. However, as follows from the schematic in Figure 9, this mechanism cannot eliminate all protrusions. Type-I and type-II protrusions cannot be overgrown and accordingly expand with increasing layer thickness. Depending on the defect density on the respective seed layer, this leads to the fact that the entire surface of the 3C-SiC layer is completely covered by protrusions at some point.

Currently, 3C-SiC wafers can be reasonably produced up to a thickness of approximately 500 μm. Figure 11 shows a 460 μm thick 3C-SiC wafer polished on both sides. Because of polishing, the protrusion defects are only visible as small black dot- or cross-like structures. For this thickness, protrusion expansion is sufficiently small so that for typical defect densities, small areas are available on the wafer in which the defect density might be sufficiently low to demonstrate technical use on a small scale. However, large-scale technical application is not practical with this material. Nevertheless, the results presented in this study point to a very promising approach that could also enable the technical use of 3C-SiC. The essential prerequisite is a considerable reduction of the

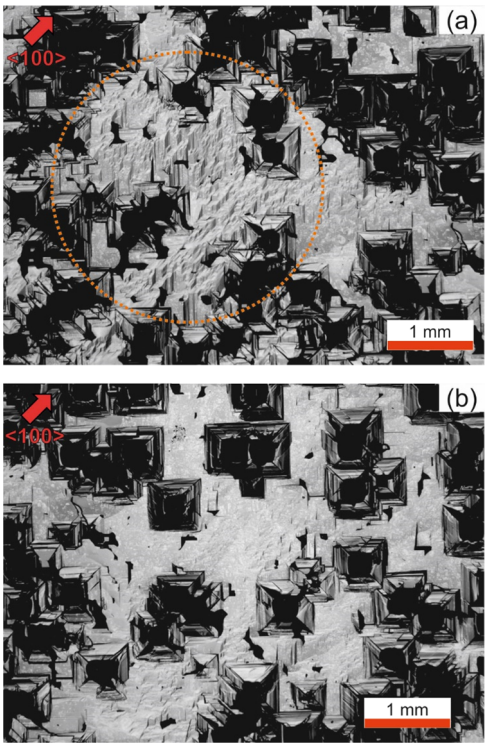

Figure 10. Surface morphology of on-axis (100)3C-SiC. (a) Local surface irregularities caused by defect accumulation that led to local substrate tilting and, accordingly, to the quasi-step-flow growth mechanism and the formation of macro steps, as indicated by circular marking. (b) On-axis growth at the smooth surface area between protrusion defects without the formation of pronounced macro steps.

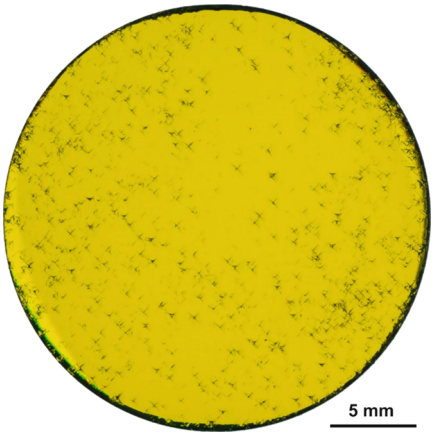

Figure 11. Transmitted light scan of a polished 1-inch 3C-SiC wafer with a thickness of (460 ± 21) μm. Polishing removed approximately 100−150 μm of the surface material on each side. The wafer shows varying protrusion densities in different areas. Protrusions are visible as black dot- or cross-shaped structures in the wafer.

https://doi.org/10.1021/acs.cgd.1c00343
Cryst. Growth Des. XXXX, XXX, XXX−XXX

protrusion defect density on the seed layers by further optimization of the CVD process. However, an appropriate, reasonable number of protrusions could be eliminated during subsequent sublimation growth, as demonstrated by the step-flow mechanism in this work. This might lead to an increase of the usable defect-free wafer area to a commercially acceptable level.

SUMMARY

The growth of 3C-SiC on free-standing off-axis 3C-SiC substrates has been demonstrated. While the surface morphology shows no change with increasing layer thickness, protrusion defects expand steadily. Depending on the defect density, the surface of the 3C-SiC layer is typically completely covered with protrusions for a layer thickness of about 2−3 mm, which prevents bulk growth and applications. For off-axis layers with a tilt toward [100], a real overgrowth mechanism for protrusion defects was found which shows the potential to significantly increase the usable area and the quality of the 3C-SiC material. The efficiency of the overgrowth mechanism depends on the structure of the protrusion. In the framework of this study, a classification of protrusions was made into three types, which show different overgrowth behaviors. The protrusions designated here as type-III can be completely overgrown through the step-flow mechanism by the surrounding high-quality material. This offers the possibility to increase the overall quality of the defective material to a certain extent by sublimation growth. Currently, protrusion defects represent the most important barrier for the technical use of the 3C-SiC material system. The results presented in this work could help overcome this obstacle.

FUNDING

This work is partially funded by the European H2020 framework program for research and innovation under grant agreement number 720827 (CHALLENGE).

AUTHOR INFORMATION

Corresponding Author

Peter Wellmann − *Crystal Growth Lab, Materials Department 6 (i-MEET), Friedrich-Alexander University Erlangen-Nürnberg (FAU), Erlangen 91058, Germany*; Email: peter.wellmann@fau.de

Authors

Michael Schöler − *Crystal Growth Lab, Materials Department 6 (i-MEET), Friedrich-Alexander University Erlangen-Nürnberg (FAU), Erlangen 91058, Germany*; orcid.org/0000-0002-5272-4954

Francesco La Via − *CNR-IMM, Sezione di Catania, Catania 95121, Italy*

Marco Mauceri − *LPE S.P.A., Catania 95121, Italy*

Complete contact information is available at: https://pubs.acs.org/10.1021/acs.cgd.1c00343

Notes

The authors declare no competing financial interest.

REFERENCES

(1) Pensl, G.; Bassler, M.; Ciobanu, F.; Afanas'ev, V.; Yano, H.; Kimoto, T.; Matsunami, H. Traps at the SiC/SiO2-interface. *Mater. Res. Soc. Symp. Proc.* **2001**, *640*, H.3.2.1−H.3.2.11.

(2) Persson, C.; Lindefelt, U. Detailed band structure for 3C-, 2H-, 4H-, 6H-SiC, and Si around the fundamental band gap. *Phys. Rev. B* **1996**, *54*, 10257−10260.

(3) Schöner, A.; Krieger, M.; Pensl, G.; Abe, M.; Nagasawa, H. Fabrication and Characterization of 3C-SiC-Based MOSFETs. *Chem. Vap. Deposition* **2006**, *12*, 523−530.

(4) Nagasawa, H.; Abe, M.; Yagi, K.; Kawahara, T.; Hatta, N. Fabrication of high performance 3C-SiC vertical MOSFETs by reducing planar defects. *Phys. Stat. Sol. (b)* **2008**, *245*, 1272−1280.

(5) Kobayashi, M.; Uchida, H.; Minami, A.; Sakata, T.; Esteve, R.; Schöner, A. 3C-SiC MOSFET with High Channel Mobility and CVD Gate Oxide. *Mater. Sci. Forum* **2011**, *679-680*, 645−648.

(6) Van Zeghbroeck, B.; Fardi, H. Comparison of 3C-SiC and 4H-SiC Power MOSFETs. *Mater. Sci. Forum* **2018**, *924*, 774−777.

(7) Tairov, Y. M.; Tsvetkov, V. F.; Lilov, S. K.; Safaraliev, G. K. Studies of growth kinetics and polytypism of silicon carbide epitaxial layers grown from the vapour phase. *J. Cryst. Growth* **1976**, *36*, 147−151.

(8) Jayatirtha, H. N.; Spencer, M. The effect of source powder height on the growth rate of 3C-SiC grown by the sublimation technique. *Inst. Phys. Conf. Ser.* **1996**, *142*, 61−64.

(9) Jayatirtha, H. N.; Spencer, M. G.; Taylor, C.; Greg, W. Improvement in the growth rate of cubic silicon carbide bulk single crystals grown by the sublimation method. *J. Cryst. Growth* **1997**, *174*, 662−668.

(10) Nishino, S.; Powell, J. A.; Will, H. A. Production of large-area single-crystal wafers of cubic SiC for semiconductor devices. *Appl. Phys. Lett.* **1983**, *42*, 460−462.

(11) Ferro, G. 3C-SiC heteroepitaxial growth on silicon: The quest for Holy Grail. *Crit. Rev. Solid State Mater. Sci.* **2015**, *40*, 56−76.

(12) La Via, F.; Severino, A.; Anzalone, R.; Bongiorno, C.; Litrico, G.; Mauceri, M.; Schoeler, M.; Schuh, P.; Wellmann, P. From thin film to bulk 3C-SiC growth: Understanding the mechanism of defects reduction. *Mater. Sci. Semicond. Process.* **2018**, *78*, 57−68.

(13) Severino, A., 3C-SiC epitaxial growth on large area Silicon: thin films. In *Silicon Carbide Epitaxy*, La Via, F., Ed. Research Signpost: Trivandrum-695 023, Kerala, India, 2012; 143−189.

(14) Severino, A.; Locke, C.; Anzalone, R.; Camarda, M.; Piluso, N.; La Magna, A.; Saddow, S.; Abbondanza, G.; D'Arrigo, G.; La Via, F. 3C-SiC Film Growth on Si Substrates. *ECS Trans.* **2019**, *7*, 312−320.

(15) Schuh, P.; La Via, F.; Mauceri, M.; Zielinski, M.; Wellmann, P. J. Growth of Large-Area, Stress-Free, and Bulk-Like 3C-SiC (100) Using 3C-SiC-on-Si in Vapor Phase Growth. *Materials* **2019**, *12*, 2179.

(16) Schuh, P.; Schöler, M.; Wilhelm, M.; Syväjärvi, M.; Litrico, G.; La Via, F.; Mauceri, M.; Wellmann, P. J. Sublimation growth of bulk 3C-SiC using 3C-SiC-on-Si (100) seeding layers. *J. Cryst. Growth* **2017**, *478*, 159−162.

(17) Schuh, P. *Sublimation Epitaxy of bulk-like Cubic Silicon Carbide*. Dissertation, Friedrich-Alexander-Universität Erlangen-Nürnberg, 2019.

(18) Jokubavicius, V.; Yazdi, G. R.; Liljedahl, R.; Ivanov, I. G.; Yakimova, R.; Syväjärvi, M. Lateral enlargement growth mechanism of 3C-SiC on off-oriented 4H-SiC substrates. *Cryst. Growth Des.* **2014**, *14*, 6514−6520.

(19) Furusho, T.; Lilov, S. K.; Ohshima, S.; Nishino, S. Effect of Tantalum in Crystal Growth of Silicon Carbide by Sublimation Close Space Technique. *Jpn. J. Appl. Phys.* **2001**, *40*, 6737−6740.

(20) Fissel, A. Thermodynamic considerations of the epitaxial growth of SiC polytypes. *J. Cryst. Growth* **2000**, *212*, 438−450.

(21) Pecholt, B.; Vendan, M.; Dong, Y.; Molian, P. Ultrafast laser micromachining of 3C-SiC thin films for MEMS device fabrication. *Int. J. Adv. Manuf. Technol.* **2008**, *39*, 239−250.

(22) Pecholt, B.; Gupta, S.; Molian, P. Review of laser microscale processing of silicon carbide. *J. Laser Appl.* **2011**, *23*, No. 012008.

(23) Camarda, M.; La Magna, A., Theoretical Monte Carlo study of the formation and evolution of defects in the homo-epitaxial growth of SiC. In *Silicon Carbide Epitaxy*, La Via, F., Ed. Research Signpost: Trivandrum-695 023, Kerala, India, 2012; 69−96.

(24) Schuh, P.; Steiner, J.; La Via, F.; Mauceri, M.; Zielinski, M.; Wellmann, P. J. Limitations during Vapor Phase Growth of Bulk (100) 3C-SiC Using 3C-SiC-on-SiC Seeding Stacks. *Materials* **2019**, *12*, 2353.
(25) Wellmann, P. J.; Schuh, P.; Kollmuss, M.; Schöler, M.; Steiner, J.; Zielinski, M.; Mauceri, M.; La Via, F. Prospects of Bulk Growth of 3C-SiC Using Sublimation Growth. *Mater. Sci. Forum* **2020**, *1004*, 113−119.
(26) Zimbone, M.; Mauceri, M.; Litrico, G.; Barbagiovanni, E. G.; Bongiorno, C.; La Via, F. Protrusions reduction in 3C-SiC thin film on Si. *J. Cryst. Growth* **2018**, *498*, 248−257.
(27) Yun, J.; Takahashi, T.; Kuroda, S.; Ishida, Y.; Okumura, H. Reduction of defects propagating into 3C-SiC homoepilayers by reactive ion etching of 3C-SiC heteroepilayer substrates. *J. Cryst. Growth* **2007**, *308*, 50−57.
(28) Yun, J.; Takahashi, T.; Mitani, T.; Ishida, Y.; Okumura, H. Reductions of twin and protrusion in 3C-SiC heteroepitaxial growth on Si(100). *J. Cryst. Growth* **2006**, *291*, 148−153.

https://doi.org/10.1021/acs.cgd.1c00343
Cryst. Growth Des. XXXX, XXX, XXX−XXX